

Dressed Quark Propagator at Finite Temperature in the Schwinger-Dyson approach with the Rainbow Approximation - exact numerical solutions and their physical implication -

Takashi Ikeda*

Department of Physics, University of Tokyo, Tokyo 113-0033, Japan
(October 23, 2018)

The Schwinger-Dyson equation for the quark in the rainbow approximation at finite temperature (T) is solved numerically without introducing any ansatz for the dressed quark propagator. The dynamical quark mass-function and the wave-function renormalization are found to have non-trivial dependence on three-momentum, Matsubara-frequency and temperature. The critical temperature of the chiral phase transition (T_c) and the T -dependence of the quark condensate are highly affected by the wave-function renormalization. We found that $T_c \simeq 155$ MeV which is consistent with the result of the finite temperature lattice QCD simulation. It is also found that the system is not a gas of free quarks but a highly interacting system of quarks and gluons even in the chirally symmetric phase.

I. INTRODUCTION

The vacuum of the quantum chromodynamics (QCD) is believed to undergo a phase transition to the chirally symmetric and deconfinement phase at high temperature and/or high baryon-density due to the asymptotic freedom and the plasma screening. Such a new state of matter is called the quark-gluon plasma (QGP) and is expected to be produced in the on-going Relativistic Heavy-Ion Collider (RHIC) at BNL and in the future Large Hadron Collider (LHC) at CERN [1]. Furthermore, in the core of the neutron stars, cold but high-density quark matter with a color superconductivity may be realized as has been extensively discussed in recent years [2].

In relation to QGP, it is of great importance to theoretically understand the phase structure of QCD at finite temperature and density [3]. The lattice QCD simulation is one of the most powerful methods for this purpose since it is based on the first principle QCD. Although the finite density simulation is still not available, the phase transition at finite T in full QCD is extensively studied on the lattice [4]. Another method, which could be potentially very useful to study the QCD phase structure, is the Schwinger-Dyson (SD) approach [5–7]. This method is based on the continuum field theory and has been applied for analysing the spontaneous chiral symmetry breaking and confinement in the vacuum. Exact SD equations are infinitely coupled integral equations and their solutions yield the n -point Euclidean Green's functions. In the practical applications, one needs to truncate the coupled SD equations by introducing some ansätze.

When one studies the spontaneous chiral symmetry breaking at zero temperature and density in the SD approach, one starts with the dressed quark propagator in the Euclidean space [5],

$$S(p) = \frac{1}{i\cancel{p}A(p^2) + B(p^2)} \equiv -i\cancel{p}\sigma_A(p^2) + \sigma_B(p^2). \quad (1.1)$$

Here, $A(p^2)$ is the wave-function renormalization and $B(p^2)$ is the quark mass-function. If one finds a solution $B(p^2) \neq 0$ in the chiral limit, it implies the spontaneous breaking of the chiral symmetry [8]. If the free gluon propagator in the Landau-gauge and the bare quark-gluon vertex are used in the 1-loop SD equation for the quark, $A(p^2) \equiv 1$ holds exactly [9,10]. However, this is not the case for other models of the gluon propagator and/or the quark-gluon vertex. The SD equation for the quark is obtained by the extremum condition of the effective potential under the variation of the dressed quark propagator S [11]. There are two distinct solutions of S in the chiral limit corresponding to the Wigner phase and the Nambu-Goldstone phase. The true ground state should be determined by calculating the effective potential in those two phases.

The introduction of temperature or baryon-density to Euclidean QCD reduces the $O(4)$ symmetry to $O(3)$. As a consequence, the dressed quark propagator in the imaginary-time formalism has a general form [5],

*ikeda@nt.phys.s.u-tokyo.ac.jp

$$\begin{aligned}
S(\mathbf{p}, \omega_n) &= \frac{1}{i\gamma \cdot \mathbf{p} A(\mathbf{p}^2, \omega_n^2) + i\gamma_4 \omega_n C(\mathbf{p}^2, \omega_n^2) + B(\mathbf{p}^2, \omega_n^2)} \\
&\equiv -i\gamma \cdot \mathbf{p} \sigma_A(\mathbf{p}^2, \omega_n^2) - i\gamma_4 \omega_n \sigma_C(\mathbf{p}^2, \omega_n^2) + \sigma_B(\mathbf{p}^2, \omega_n^2).
\end{aligned} \tag{1.2}$$

Here $\omega_n = (2n+1)\pi T + i\mu$ ($n \in \mathbb{Z}$) is the Matsubara-frequency for the quark. T and μ are the temperature and the quark chemical potential respectively. $A(\mathbf{p}^2, \omega_n^2)$ and $C(\mathbf{p}^2, \omega_n^2)$ represent the quark wave-function renormalization, and $B(\mathbf{p}^2, \omega_n^2)$ is the quark mass-function. For $T \neq 0$ and/or $\mu \neq 0$, $A(\mathbf{p}^2, \omega_n^2) = C(\mathbf{p}^2, \omega_n^2) = 1$ does NOT hold even if the free gluon propagator in the Landau-gauge and the bare quark-gluon vertex are used in the 1-loop SD equation.

The purpose of this paper is to obtain a dressed quark propagator at $T \neq 0$ by solving the 1-loop SD equation for the quark without any ansatz for the functions A , C and B , and to investigate their physical implications. The exact numerical solutions of A , C and B have explicit $(\mathbf{p}^2, \omega_n^2)$ dependences. Although such functions have been obtained in a simple model where the SD equation can be solved algebraically [5], the $(\mathbf{p}^2, \omega_n^2)$ dependence of A and C for realistic models such as QCD-like theory [12] has not been known. Non-trivial $(\mathbf{p}^2, \omega_n^2)$ dependence of the functions A and C to the nonperturbative phenomena of QCD in the Wigner phase will be also discussed.

The paper is organized as follows. In Sec. II. A, the SD equation and the CJT effective potential for the quark are summarized. Then a model for the gluon propagator, the quark-gluon vertex and the QCD coupling constant is introduced at $T = 0$. In Sec. II. B, they are extended to $T \neq 0$. In Sec. III, basic parameters of the model introduced in Sec. II are determined by the condition $f_\pi = 93$ MeV at $T = 0$. Then the quark wave-function renormalization $A(\mathbf{p}^2, \omega_n^2)$ and $C(\mathbf{p}^2, \omega_n^2)$ and the quark mass-function $B(\mathbf{p}^2, \omega_n^2)$ are obtained self-consistently at $T \neq 0$ by solving the SD equation with simultaneous iteration. By calculating the effective potential corresponding to those solutions, the true ground state is determined at given T . The critical temperature T_c at which the chiral symmetry is restored is also obtained. The effect of the $(\mathbf{p}^2, \omega_n^2)$ dependence of A and C on the chiral phase transition is examined. In Sec. IV conclusions and discussions are given. In Appendix, the explicit forms of the integral kernels which appear in the SD equation for the quark are given. In this paper, massless (u,d)-quarks are considered, and all calculations are done in the imaginary-time formalism [13].

II. SD EQUATION AND EFFECTIVE POTENTIAL

A. SD eq. for the quark at $T = 0$ in the rainbow approximation and the CJT effective potential

At $T = 0$, the SD equation for the quark in the chiral limit is expressed as,

$$S^{-1}(p) = S_{(0)}^{-1}(p) + \Sigma(p). \tag{2.1}$$

Here, $S(p)$ and $S_{(0)}(p)$ are the dressed quark propagator in eq. (1.1) and the free quark propagator $1/i\gamma$ in the chiral limit, respectively. $\Sigma(p_\mu)$ represents the self-energy of the quark. Eq. (2.1) is derived by the extremum condition for the CJT effective potential $V[S]$ under the variation of $S(p)$ [11];

$$V[S] = V_1[S] + V_2[S], \tag{2.2}$$

$$V_1[S] = \int \frac{d^4 p}{(2\pi)^4} \text{tr} \left\{ \ln \left[S_{(0)}^{-1}(p) S(p) \right] - S_{(0)}^{-1}(p) S(p) + 1 \right\}, \tag{2.3}$$

$$V_2[S] = -\frac{1}{2} \int \frac{d^4 p}{(2\pi)^4} \{ \text{tr} [\Sigma(p) S(p)] \}. \tag{2.4}$$

Here “tr” is taken over the Dirac, flavor and color matrices. $V_1[S]$ corresponds to the 1-loop potential with the quark 1-loop diagram and $V_2[S]$ is the 2-loop potential with the one gluon exchange. $\Sigma(p^2)$ has a general form;

$$\Sigma(p) = \int \frac{d^4 k}{(2\pi)^4} g \frac{\lambda^a}{2} \gamma_\mu S(k^2) g \Gamma_\nu^a(p, k) D_{\mu\nu}(p - k), \tag{2.5}$$

where $\Gamma_\nu^a(p, k)$ and $D_{\mu\nu}(p - k)$ are the dressed quark-gluon vertex function and the dressed gluon propagator respectively.

Eq. (2.1) can be decomposed into two coupled integral equations for $A(p^2)$ and $B(p^2)$ by taking the trace “Tr” over the gamma matrices [5,14];

$$A(p^2) = 1 - \frac{i}{4p^2} \text{Tr} [\not{p} \Sigma(p)], \quad (2.6)$$

$$B(p^2) = \frac{1}{4} \text{Tr} [\Sigma(p)]. \quad (2.7)$$

Since $\Sigma(p)$ contains the dressed quark propagator, right-hand sides of eqs. (2.6) and (2.7) are implicit functions of $A(k^2)$ and $B(k^2)$ integrated over the momentum k . Once one obtains the solutions $A(p^2)$ and $B(p^2)$, the effective potential corresponding to those solutions are given by

$$\begin{aligned} V[S] &= -4N_c \int \frac{d^4 p}{(2\pi)^4} \left\{ \ln(p^2 A^2(p^2) + B^2(p^2)) + p^2 \sigma_A(p^2) - \ln p^2 - 1 \right\} \\ &= -\frac{N_c}{\pi^3} \int_{-\infty}^{\infty} dp_4 \int_0^{\infty} d|\mathbf{p}| p^2 \left\{ \ln((\mathbf{p}^2 + p_4^2) A^2(\mathbf{p}^2, p_4^2) + B^2(\mathbf{p}^2, p_4^2)) \right. \\ &\quad \left. + (\mathbf{p}^2 + p_4^2) \sigma_A(\mathbf{p}^2, p_4^2) - \ln(\mathbf{p}^2 + p_4^2) - 1 \right\}. \end{aligned} \quad (2.8)$$

To make the connection to $T \neq 0$ case clear, the integration over the 4-momentum are decomposed into $|\mathbf{p}|$ and p_4 instead of $p^2 = \mathbf{p}^2 + p_4^2$ in eq. (2.8). In eq. (2.8) the factor 2 for the degenerate (u, d)-quark is included explicitly.

In order to solve eqs. (2.6) and (2.7) in terms of $A(\mathbf{p}^2, p_4^2)$ and $B(\mathbf{p}^2, p_4^2)$, one needs to define the structure of the dressed gluon propagator $D_{\mu\nu}$, the dressed quark-gluon vertex function Γ_μ^a and the coupling constant g^2 . In this paper we adopt the following model: For the dressed quark-gluon vertex function, we use the rainbow approximation $\Gamma_\mu^a(p, k) = \frac{\lambda^a}{2} \gamma_\mu$, where λ^a is the color Gell-Mann matrices. For the coupling constant g^2 , the QCD running coupling constant in the one-loop order with an infrared regulator p_c is used to describe the momentum dependence [15];

$$\frac{g^2(p^2)}{4\pi} = \frac{4\pi}{9} \frac{1}{\ln[(p^2 + p_c^2)/\Lambda_{\text{QCD}}^2]}. \quad (2.9)$$

p_c approximately divides the momentum scale into the infrared region and the ultraviolet region. Furthermore, we adopt the Higashijima-Miransky approximation [16,17] for the QCD running coupling constant

$$g^2((p - k)^2) = \theta(p^2 - k^2) g^2(p^2) + \theta(k^2 - p^2) g^2(k^2) = g^2(\max[p^2, k^2]). \quad (2.10)$$

In this approximation the quark mass-function $B(p^2)$ in the ultraviolet region has an asymptotic form consistent with that obtained by the operator product expansion and the renormalization group. For the dressed gluon propagator, we use the free one $D_{\mu\nu}^{(0)}(p - k)$ in the Landau-gauge,

$$D_{\mu\nu}^{(0)}(p) = \left(\delta_{\mu\nu} - \frac{p_\mu p_\nu}{p^2} \right) \frac{1}{p^2}. \quad (2.11)$$

The Landau-gauge is a fixed point of the renormalization group and the gauge parameter is zero to all orders in perturbation theory [18].

The integration over the angle between p and k can be performed in (2.5) because the running coupling constant has no angle dependence. Then the quark self-energy has no term with odd number of γ_μ , that is $\text{Tr}[\not{p} \Sigma(p)] = 0$. As a consequence, eq. (2.6) reduces to $A(p^2) = 1$ in this model as mentioned in Sec. I. The SD equation for the quark becomes a single integral equation (2.7) for $B(p^2)$ after integrating over the angle between p and k ,

$$B(p^2) = \frac{3C_F}{16\pi^2} \int dk^2 \frac{g^2(\max[p^2, k^2])}{\max[p^2, k^2]} \cdot \frac{k^2 B(k^2)}{k^2 + B^2(k^2)}, \quad (2.12)$$

where $C_F = (N_c^2 - 1)/2N_c$ is the quadratic Casimir operator for the color $\text{SU}(N_c)$ group. Eq. (2.12) can be expressed in term of the variables \mathbf{p} and p_4 instead of $p^2 = \mathbf{p}^2 + p_4^2$,

$$B(\mathbf{p}^2, p_4^2) = \int_{-\infty}^{\infty} dk_4 \int_0^{\infty} d|\mathbf{k}| \frac{\mathbf{k}^2 B(\mathbf{k}^2, k_4^2)}{\mathbf{k}^2 + k_4^2 + B^2(\mathbf{k}^2, k_4^2)} \cdot E_1(|\mathbf{p}|, p_4; |\mathbf{k}|, k_4). \quad (2.13)$$

The explicit form of $E_1(|\mathbf{p}|, p_4; |\mathbf{k}|, k_4)$ is given in Appendix. Eq. (2.13) has two distinct solutions; one is a trivial solution $B_W(\mathbf{p}^2, p_4^2) = 0$ representing a free quark, and another is a non-trivial solution $B_{NG}(\mathbf{p}^2, p_4^2) \neq 0$. The subscript W represents the “Wigner” solution describing a phase in which the chiral symmetry is not broken. The subscript NG represents the “Nambu-Goldstone” (NG) solution which represents a phase in which the chiral symmetry is broken spontaneously. To determine the true ground state realized at $T = 0$, the effective potential $V[S]$ with the Wigner solution and that with the NG solution have to be compared.

B. SD eq. for the quark at $T \neq 0$

In this subsection, we extend the formulas in the previous subsection to $T \neq 0$. For this purpose, we apply the imaginary time formalism [13] and make a replacement

$$\int \frac{d^4 p}{(2\pi)^4} f(\mathbf{p}, p_4) \rightarrow T \sum_{n=-\infty}^{\infty} \int \frac{d^3 \mathbf{p}}{(2\pi)^3} f(\mathbf{p}, \omega_n), \quad (2.14)$$

where $\omega_n = (2n+1)\pi T$ ($n \in \mathbb{Z}$) is the Matsubara-frequency for the fermion. The SD equation for the quark (2.1) at $T \neq 0$ is decomposed into three coupled integral equations for $A(\mathbf{p}^2, \omega_n^2)$, $C(\mathbf{p}^2, \omega_n^2)$ and $B(\mathbf{p}^2, \omega_n^2)$:

$$\begin{aligned} B(\mathbf{p}^2, \omega_n^2) &= C_F T \sum_{m=-\infty}^{\infty} \int \frac{d^3 \mathbf{k}}{(2\pi)^3} g^2 (\max[\mathbf{p}^2 + \omega_n^2, \mathbf{k}^2 + \omega_m^2]) \\ &\quad \times \frac{B(\mathbf{k}^2, \omega_m^2)}{\mathbf{k}^2 A^2(\mathbf{k}^2, \omega_m^2) + \omega_m^2 C^2(\mathbf{k}^2, \omega_m^2) + B^2(\mathbf{k}^2, \omega_m^2)} D_{\mu\mu}^{(0)}(\mathbf{p} - \mathbf{k}, \omega_n - \omega_m), \end{aligned} \quad (2.15)$$

$$\begin{aligned} A(\mathbf{p}^2, \omega_n^2) &= 1 - \frac{C_F}{\mathbf{p}^2} T \sum_{m=-\infty}^{\infty} \int \frac{d^3 \mathbf{k}}{(2\pi)^3} \cdot \frac{g^2 (\max[\mathbf{p}^2 + \omega_n^2, \mathbf{k}^2 + \omega_m^2])}{\mathbf{k}^2 A^2(\mathbf{k}^2, \omega_m^2) + \omega_m^2 C^2(\mathbf{k}^2, \omega_m^2) + B^2(\mathbf{k}^2, \omega_m^2)} \\ &\quad \times \left\{ A(\mathbf{k}^2, \omega_m^2) \left[2p_j k_i D_{ji}^{(0)}(\mathbf{p} - \mathbf{k}, \omega_n - \omega_m) - \mathbf{p} \cdot \mathbf{k} D_{\mu\mu}^{(0)}(\mathbf{p} - \mathbf{k}, \omega_n - \omega_m) \right] \right. \\ &\quad \left. + 2C(\mathbf{k}^2, \omega_m^2) \omega_m p_j D_{4j}^{(0)}(\mathbf{p} - \mathbf{k}, \omega_n - \omega_m) \right\}, \end{aligned} \quad (2.16)$$

$$\begin{aligned} C(\mathbf{p}^2, \omega_n^2) &= 1 - \frac{C_F}{\omega_n} T \sum_{m=-\infty}^{\infty} \int \frac{d^3 \mathbf{k}}{(2\pi)^3} \cdot \frac{g^2 (\max[\mathbf{p}^2 + \omega_n^2, \mathbf{k}^2 + \omega_m^2])}{\mathbf{k}^2 A^2(\mathbf{k}^2, \omega_m^2) + \omega_m^2 C^2(\mathbf{k}^2, \omega_m^2) + B^2(\mathbf{k}^2, \omega_m^2)} \\ &\quad \times \left\{ 2A(\mathbf{k}^2, \omega_m^2) k_j D_{4i}^{(0)}(\mathbf{p} - \mathbf{k}, \omega_n - \omega_m) \right. \\ &\quad \left. + \omega_m C(\mathbf{k}^2, \omega_m^2) \left[2D_{44}^{(0)}(\mathbf{p} - \mathbf{k}, \omega_n - \omega_m) - D_{\mu\mu}^{(0)}(\mathbf{p} - \mathbf{k}, \omega_n - \omega_m) \right] \right\}. \end{aligned} \quad (2.17)$$

By making the integration over the angle between \mathbf{p} and \mathbf{k} , eqs. (2.15), (2.16) and (2.17) reduce to the following equations:

$$B(\mathbf{p}^2, \omega_n^2) = 2\pi T \sum_{m=-\infty}^{\infty} \int d|\mathbf{k}| \frac{\mathbf{k}^2 B(\mathbf{k}^2, \omega_m^2)}{\mathbf{k}^2 A^2(\mathbf{k}^2, \omega_m^2) + \omega_m^2 C^2(\mathbf{k}^2, \omega_m^2) + B^2(\mathbf{k}^2, \omega_m^2)} \cdot E_1(|\mathbf{p}|, \omega_n; |\mathbf{k}|, \omega_m), \quad (2.18)$$

$$\begin{aligned} A(\mathbf{p}^2, \omega_n^2) &= 1 + \frac{2\pi T}{\mathbf{p}^2} \sum_{m=-\infty}^{\infty} \int d|\mathbf{k}| \frac{\mathbf{k}^2}{\mathbf{k}^2 A^2(\mathbf{k}^2, \omega_m^2) + \omega_m^2 C^2(\mathbf{k}^2, \omega_m^2) + B^2(\mathbf{k}^2, \omega_m^2)} \\ &\quad \times \left\{ A(\mathbf{k}^2, \omega_m^2) E_2(|\mathbf{p}|, \omega_n; |\mathbf{k}|, \omega_m) + \omega_m C(\mathbf{k}^2, \omega_m^2) E_3(|\mathbf{p}|, \omega_n; |\mathbf{k}|, \omega_m) \right\}, \end{aligned} \quad (2.19)$$

$$\begin{aligned} C(\mathbf{p}^2, \omega_n^2) &= 1 + \frac{2\pi T}{\omega_n} \sum_{m=-\infty}^{\infty} \int d|\mathbf{k}| \frac{\mathbf{k}^2}{\mathbf{k}^2 A^2(\mathbf{k}^2, \omega_m^2) + \omega_m^2 C^2(\mathbf{k}^2, \omega_m^2) + B^2(\mathbf{k}^2, \omega_m^2)} \\ &\quad \times \left\{ A(\mathbf{k}^2, \omega_m^2) E_4(|\mathbf{p}|, \omega_n; |\mathbf{k}|, \omega_m) + \omega_m C(\mathbf{k}^2, \omega_m^2) E_5(|\mathbf{p}|, \omega_n; |\mathbf{k}|, \omega_m) \right\}. \end{aligned} \quad (2.20)$$

Explicit forms of $E_i(|\mathbf{p}|, \omega_n; |\mathbf{k}|, \omega_m)$ ($i = 1, 2, 3, 4, 5$) are given in Appendix. Eq. (2.18) may have two distinct solutions: $B = B_W(\mathbf{p}^2, \omega_n^2) = 0$ and $B = B_{NG}(\mathbf{p}^2, \omega_n^2) \neq 0$. We call the solutions of eqs. (2.19) and (2.20) corresponding to B_W as (A_W, C_W) and to B_{NG} as (A_{NG}, C_{NG}) . The dressed quark propagators in the Wigner phase and the NG phase are defined by

$$\begin{aligned} S_W(\mathbf{p}, \omega_n) &\equiv \frac{1}{i\gamma \cdot \mathbf{p} A_W(\mathbf{p}^2, \omega_n^2) + i\gamma_4 \omega_n C_W(\mathbf{p}^2, \omega_n^2)} \\ &\equiv -i\gamma \cdot \mathbf{p} \sigma_{A_W}(\mathbf{p}^2, \omega_n^2) - i\gamma_4 \omega_n \sigma_{C_W}(\mathbf{p}^2, \omega_n^2), \end{aligned} \quad (2.21)$$

$$\begin{aligned} S_{NG}(\mathbf{p}, \omega_n) &\equiv \frac{1}{i\gamma \cdot \mathbf{p} A_{NG}(\mathbf{p}^2, \omega_n^2) + i\gamma_4 \omega_n C_{NG}(\mathbf{p}^2, \omega_n^2) + B_{NG}(\mathbf{p}^2, \omega_n^2)} \\ &\equiv -i\gamma \cdot \mathbf{p} \sigma_{A_{NG}}(\mathbf{p}^2, \omega_n^2) - i\gamma_4 \omega_n \sigma_{C_{NG}}(\mathbf{p}^2, \omega_n^2) + \sigma_{B_{NG}}(\mathbf{p}^2, \omega_n^2). \end{aligned} \quad (2.22)$$

Unlike the case at $T = 0$, the quark self-energy $\Sigma(\mathbf{p}^2, \omega_n^2)$ can have terms with odd powers of γ_μ at $T \neq 0$. Therefore, A and C cannot be equal to unity even when we take the rainbow approximation with the free gluon propagator in the Landau-gauge. Furthermore, A and C have non-trivial dependence on \mathbf{p}^2 and ω_n^2 .¹

Once one obtains A, C and B , the effective potential at $T \neq 0$ as a direct generalization of eq. (2.14) can be calculated through the formula,

$$V[S] = -\frac{2N_c}{\pi^2} T \sum_{n=-\infty}^{\infty} \int d|\mathbf{p}| \mathbf{p}^2 \left\{ \ln (\mathbf{p}^2 A^2(\mathbf{p}^2, \omega_n^2) + \omega_n^2 C^2(\mathbf{p}^2, \omega_n^2) + B^2(\mathbf{p}^2, \omega_n^2)) \right. \\ \left. + \mathbf{p}^2 \sigma_A(\mathbf{p}^2, \omega_n^2) + \omega_n^2 \sigma_C(\mathbf{p}^2, \omega_n^2) - \ln (\mathbf{p}^2 + \omega_n^2) - 1 \right\}. \quad (2.23)$$

To study the chiral phase transition, the difference of the free energy between the NG phase ($B_{NG} \neq 0$) and the Wigner phase ($B_W = 0$) should be considered:

$$\bar{V}(T) \equiv V[S_{NG}] - V[S_W] \\ = -\frac{2N_c}{\pi^2} T \sum_{n=-\infty}^{\infty} \int d|\mathbf{p}| \mathbf{p}^2 \left\{ \ln \left[\frac{\mathbf{p}^2 A_{NG}^2(\mathbf{p}^2, \omega_n^2) + \omega_n^2 C_{NG}^2(\mathbf{p}^2, \omega_n^2) + B_{NG}^2(\mathbf{p}^2, \omega_n^2)}{\mathbf{p}^2 A_W^2(\mathbf{p}^2, \omega_n^2) + \omega_n^2 C_W^2(\mathbf{p}^2, \omega_n^2)} \right] \right. \\ \left. + \mathbf{p}^2 [\sigma_{A_{NG}}(\mathbf{p}^2, \omega_n^2) - \sigma_{A_W}(\mathbf{p}^2, \omega_n^2)] + \omega_n^2 [\sigma_{C_{NG}}(\mathbf{p}^2, \omega_n^2) - \sigma_{C_W}(\mathbf{p}^2, \omega_n^2)] \right\}. \quad (2.24)$$

If $\bar{V}(T) > 0 (< 0)$, the chiral symmetry is restored (spontaneously broken).

III. CHIRAL PHASE TRANSITION AT FINITE TEMPERATURE

A. Determination of the parameters at $T = 0$

In this subsection, we determine the parameters of the model in Sec. II. A at $T = 0$. First of all, the momentum integrals in eqs. (2.8) and (2.13) are regulated by the ultraviolet cutoff Λ . As far as Λ is large enough, physical quantities such as f_π and $V[S]$ do not depend on Λ , while the Λ -dependence of the chiral condensate $\langle \bar{q}q \rangle_\Lambda$ is governed by the renormalization group equation. In our numerical calculation, we adopt $\Lambda = 5.42$ GeV above which f_π and $V[S]$ are insensitive to Λ .

The chiral condensate $\langle \bar{q}q \rangle_\Lambda$ is known to be insensitive to the infrared regularization parameter p_c [12]. Therefore we take $p_c^2/\Lambda_{QCD}^2 = e^{0.1}$ and determine Λ_{QCD} to reproduce the pion decay constant $f_\pi = 93$ MeV [12]. As mentioned in Sec. II. A, eq. (2.13) has two distinct solutions. One is a trivial solution $B_W(\mathbf{p}^2, p_4^2) = 0$ corresponding to the free quark. For this solution, $f_\pi = 0$ and $\langle \bar{q}q \rangle_\Lambda = 0$. Another solution is $B_{NG}(\mathbf{p}^2, p_4^2) \neq 0$ which represents the spontaneous chiral symmetry breaking. This solution is obtained by solving eq. (2.13) numerically by iteration, starting from an arbitrary given trial function $B_{\text{trial}}(\mathbf{p}^2, p_4^2) \neq 0$. In this case, f_π can be calculated from the formula [19],

$$f_\pi N_\pi = \frac{N_c}{\pi^3} \int_{-\Lambda}^{\Lambda} dp_4 \int_0^{\Lambda} d|\mathbf{p}| \mathbf{p}^2 B(\mathbf{p}^2, p_4^2) \left\{ \sigma_A \sigma_B + \frac{2}{3} \mathbf{p}^2 (\sigma'_A \sigma_B + \sigma_A \sigma'_B) \right\}, \quad (3.1)$$

with $\sigma'_B \equiv \partial \sigma_B(\mathbf{p}^2, p_4^2) / \partial \mathbf{p}^2$ and $\sigma'_A \equiv \partial \sigma_A(\mathbf{p}^2, p_4^2) / \partial \mathbf{p}^2$. N_π is a canonical normalization constant for the Bethe-Salpeter amplitude in the ladder approximation,

$$N_\pi^2 = \frac{N_c}{2\pi^3} \int_{-\Lambda}^{\Lambda} dp_4 \int_0^{\Lambda} d|\mathbf{p}| \mathbf{p}^2 B^2(\mathbf{p}^2, p_4^2) \left\{ \sigma_A^2 - 2 [\mathbf{p}^2 \sigma_A \sigma'_A + p_4^2 \sigma_C \sigma'_C + \sigma_B \sigma'_B] \right. \\ \left. - \frac{4}{3} \mathbf{p}^2 \left[\mathbf{p}^2 (\sigma_A \sigma''_A - (\sigma'_A)^2) + p_4^2 (\sigma_C \sigma''_C - (\sigma'_C)^2) + \sigma_B \sigma''_B - (\sigma'_B)^2 \right] \right\}, \quad (3.2)$$

¹In a simple algebraically soluble model, it was noted before that this non-trivial dependence has significant effect on the bulk thermodynamic quantities [5].

with $\sigma'_C \equiv \partial\sigma_C(\mathbf{p}^2, p_4^2)/\partial\mathbf{p}^2 = \sigma'_A$ at $T = 0$. If $A = C = 1$, one obtains $N_\pi = f_\pi$ [19], and $\Lambda_{\text{QCD}} = 734$ MeV is determined by the input $f_\pi = 93$ MeV in eqs. (3.1) or (3.2) with $A = C = 1$ and B_{NG} . Our parameters are consistent with those obtained in [12].

The effective potential for the solution B_{NG} is obtained from eq. (2.8). The difference of the vacuum energy between the NG phase and the Wigner phase reads $\bar{V}(0) = -(172.7 \text{ MeV})^4 < 0$. This means that the state corresponding to the NG solution is realized at $T = 0$. At the scale Λ , the chiral condensate $\langle\bar{q}q\rangle_\Lambda$ is calculated as

$$\begin{aligned}\langle\bar{q}q\rangle_\Lambda &= - \int_{-\Lambda}^{\Lambda} \frac{d^4 p}{(2\pi)^4} \text{tr}[S(p)] \\ &= -\frac{3}{\pi^3} \int_{-\Lambda}^{\Lambda} dp_4 \int_0^{\Lambda} d|\mathbf{p}| \mathbf{p}^2 \sigma_B(\mathbf{p}^2, p_4^2).\end{aligned}\quad (3.3)$$

With the parameter set determined above, we obtain $\langle\bar{q}q\rangle_\Lambda = (-293 \text{ MeV})^3$. If we change the scale from Λ to 1 GeV by the perturbative renormalization group equation, $\langle\bar{q}q\rangle_{1\text{GeV}} = (-217 \text{ MeV})^3$ is obtained, which is consistent with the known phenomenological value.

B. The exact numerical solutions of the SD eq. in the rainbow approximation at $T \neq 0$

At $T \neq 0$, we need to replace the dp_4 integral by the Matsubara sum,

$$\int_{-\Lambda}^{\Lambda} \frac{dp_4}{2\pi} f(\mathbf{p}, p_4) \rightarrow T \sum_{n=-n_{\text{max}}}^{n_{\text{max}}} f(\mathbf{p}, \omega_n), \quad (3.4)$$

with n_{max} being the largest integer n satisfying $\omega_n = (2n+1)\pi T \leq \Lambda$. In order to study how the quark wave-function renormalization affects the nature of the chiral phase transition, eqs. (2.18), (2.19) and (2.20) are solved in two different cases with the parameter set determined at $T = 0$.

- (I) : A and C are assumed to be 1 and only eq. (2.18) for B is solved numerically. The trivial solution $B = 0$ of eq. (2.18) corresponds to the free quark and the numerical solution $B_{NG} \neq 0$ corresponds to the phase of the spontaneous chiral symmetry breaking. We define the difference of the free energy between the NG phase and the Wigner phase in this case as $\bar{V}_{(I)}(T)$ according to eq. (2.24) with $A_W = C_W = A_{NG} = C_{NG} = 1$.
- (II) : Three coupled eqs. (2.18), (2.19) and (2.20) are solved numerically with initial trial functions for A, B and C . We call the solutions corresponding to the Wigner phase as $B_W (= 0), A_W (\neq 1)$ and $C_W (\neq 1)$ while those corresponding to the NG phase as $B_{NG} (\neq 0), A_{NG} (\neq 1)$ and $C_{NG} (\neq 1)$. The difference of the free energy between the NG phase and the Wigner phase is defined as $\bar{V}_{(II)}(T)$ according to eq. (2.24).

Fig. 1 shows the momentum dependence of the quark mass-function $B_{NG}(\mathbf{p}^2, \omega_0^2)$ in the case (I) with a zeroth Matsubara-frequency $\omega_0 = \pi T$ at $T = 10, 150, 200$ and 216 MeV. $B_{NG}(\mathbf{p}^2, \omega_n^2)$ in the low momentum region decreases with the increase of $|n|$ at given T . For $T \geq 217$ MeV, eq. (2.18) have only the trivial solution $B_W = 0$.

Fig. 2 (a) and (b) show the momentum dependence of the functions A_W and C_W in the case (II) with $\omega_0 = \pi T$. It is found that A_W and C_W in the low momentum region do not reach unity even at $T \sim$ a few hundred MeV. This implies that the quarks and gluons are strongly interacting even in the high T chirally symmetric phase. For $\omega_n (n \neq 0)$, the difference of A_W and C_W from unity decreases with the increase of $|n|$ at given T .

The momentum dependence of the quark mass-function B_{NG} in the case (II) with $\omega_0 = \pi T$ is shown in Fig. 3. The non-trivial solution $B_{NG} \neq 0$ is obtained only below $T = 155$ MeV and eq. (2.18) have only a trivial solution $B_W = 0$ for $T \geq 155$ MeV. B_{NG} for $\omega_n (n \neq 0)$ in the low momentum region becomes smaller as $|n|$ increases at given T .

Fig. 4 (a) and (b) show the momentum dependence of the functions A_{NG} and C_{NG} with $\omega_0 = \pi T$. It is found that the difference of A_{NG} and C_{NG} from unity in the low momentum region is maximal around $T = 150$ MeV, and then A_{NG} and C_{NG} coincide with A_W and C_W for $T \geq 155$ MeV. For $\omega_n (n \neq 0)$, the difference of A_{NG} and C_{NG} from unity decreases with the increase of $|n|$ at given T .

As mentioned before, in order to determine the critical temperature T_c of the chiral symmetry restoration, one has to calculate the difference of the effective potential between the NG phase and the Wigner phase, $\bar{V}(T)$ in eq. (2.24). T_c is defined by the temperature at which $\bar{V}(T_c) = 0$. Fig. 5 shows the T -dependence of $\bar{V}_{(I)}(T)$ and $\bar{V}_{(II)}(T)$. It is found that $T_c = 217$ MeV in the case (I) and $T_c = 155$ MeV in the case (II), and the chiral phase transition is of the second order in both cases. Due to the crude ansatz $A = C = 1$ at $T \neq 0$ in the case (I), $\bar{V}_{(I)}(T)$ has a strange

behavior in which it decreases first and then increases as T increases. Such behavior disappears in $\bar{V}_{(II)}(T)$ where A and C are solved together with B . $\bar{V}_{(II)}(T)$ increases monotonically as T increases and vanishes at T_c .

The pion decay constant f_π at $T \neq 0$ is obtained from eqs. (3.1) and (3.2) using eq. (3.4). Fig. 6 shows the T -dependence of f_π for the NG solution in the case (I) and (II). In the case (I), f_π has a strange behavior in which it increases first and then decreases as T increases because of the crude approximation $A = C = 1$. This behavior is correlated with that of $\bar{V}_{(I)}(T)$ in Fig. 5. On the other hand, f_π in the case (II) decreases slowly first and then changes suddenly near T_c as T increases. The chiral condensate $\langle\bar{q}q\rangle_\Lambda$ at the scale Λ are calculated by eq.(3.3) using eq.(3.4) at $T \neq 0$. In Fig. 7, the T -dependence of $\langle\bar{q}q\rangle_\Lambda$ for the NG solution in the case (I) and (II) is shown. For the same reason as that in f_π , the strange behavior of $\langle\bar{q}q\rangle_\Lambda$ in the case (I) is found, while $\langle\bar{q}q\rangle_\Lambda$ in the case (II) has an almost constant value first and then decreases suddenly near T_c as T increases.

As mentioned above, the phase transitions in (I) and in (II) are both of the second order, so the critical exponents can be defined. Fig. 8 shows the scaling behaviour of $\langle\bar{q}q\rangle_\Lambda$ in (I) and in (II) near the critical temperature in each case. The critical exponent β is defined by

$$\langle\bar{q}q\rangle_\Lambda \sim \left(1 - \frac{T}{T_c}\right)^\beta \quad \text{for } T \rightarrow T_c - 0. \quad (3.5)$$

β is determined by using the linear-log fit numerically as follows

$$\ln\langle\bar{q}q\rangle_\Lambda = \beta \ln\left(1 - \frac{T}{T_c}\right) + \text{const.}, \quad (3.6)$$

where const. is independent of T . We find that $\beta \sim 0.51$ in (I) and ~ 0.53 in (II) respectively. Both values are consistent with β in the mean-field theory and agrees with ref. [12,20]. The mean-field critical exponents are a result of the structure of the gap equation for the fermion. The inclusion of the soft collective modes will move the mean field exponents to the $O(4)$ values as expected from the renormalization group argument [3].

IV. CONCLUSIONS AND DISCUSSIONS

In this paper, we have obtained the dressed quark propagator as the numerical solutions by solving the SD eq. for the quark without any ansatz and studied the effect of the quark wave-function renormalization on the chiral phase transition at $T \neq 0$. The SD eq. for the quark has been solved at one-loop level. We use the free gluon propagator in the Landau-gauge, the bare quark-gluon vertex, the one-loop QCD running coupling with the infrared regulator and Higashijima-Miransky approximation. The three-momentum and Matsubara-frequency dependent functions for the quark wave-function renormalization differ from unity especially in the low momentum region. As a result the critical temperature decreases substantially compared to that with $A = C = 1$.

To examine the effect of the quark wave-function renormalization, we have solved the SD eq. for the quark in two cases:

(I) : the SD eq. for B is solved with an assumption $A = C = 1$.

(II) : coupled SD eq. for A, B and C are solved numerically.

(I) is an approximate solution, and (II) is the exact solutions of the SD eq. for the quark. The Wigner solution in the case (I) corresponds to the free quark. From the difference of the free energy between the NG phase and the Wigner phase in the case (I), the critical temperature of the chiral phase transition turns out to be $T_c = 217$ MeV. Also the difference of the free energy between the NG phase and the Wigner phase in the case (II) shows $T_c = 155$ MeV. Exact numerical solution with $A \neq 1 \neq C$ in the case (II) not only reduces the critical temperature but also removes the pathological behavior of f_π and $\langle\bar{q}q\rangle$ in the case (I). We found that after the chiral symmetry restoration, quarks are not free even at temperature of a few hundred MeV in the case (II). In both cases (I) and (II), the chiral phase transition is of the second order. The critical exponent β is extracted from $\langle\bar{q}q\rangle$ near T_c and we obtained $\beta \sim 0.51$ in (I) and $\beta \sim 0.53$ in (II). They are consistent with the result of [5,12,20].

Finally, several comments are in order. The gluon propagator used in this paper is the free one and cannot explain the quark and gluon confinement. To study the effect of the quark confinement on the chiral phase transition, it would be necessary to use the phenomenological gluon propagator such as the dual Ginzburg-Landau model which explains the spontaneous chiral symmetry breaking and the quark confinement [21,22]. The screening of the gluon should be also included. The electric sector of the gluon propagator is influenced by the Debye screening and the magnetic sector by the non-perturbative magnetic mass in the static case or the dynamical screening in the non static case. The study

of the chiral phase transition at finite density and temperature is also an important future problem in our approach to locate the tricritical point in the QCD phase diagram [23]. Our preliminary study shows that the location of the tricritical point in our model is $(T_{tr}, \mu_{tr}^B) = (210 \text{ MeV}, 129 \text{ MeV})$ for the case (I) and $(142 \text{ MeV}, 246 \text{ MeV})$ for the case (II), where $\mu_{tr}^B (= 3\mu_{tr})$ is the baryon chemical potential.

ACKNOWLEDGEMENTS

I am grateful to T. Hatsuda and S. Sasaki for their stimulating discussions, comments and encouragement.

APPENDIX:

In this appendix, we show explicit forms of five kernels $E_i(|\mathbf{p}|, \omega_n; |\mathbf{k}|, \omega_m)$ ($i = 1, 2, 3, 4, 5$) in eqs. (2.7), (2.18), (2.19) and (2.20):

$$E_1(|\mathbf{p}|, \omega_n; |\mathbf{k}|, \omega_m) = -\frac{4}{9\pi|\mathbf{p}||\mathbf{k}|} \cdot \frac{1}{\ln \left[(\max[\mathbf{p}^2 + \omega_n^2, \mathbf{k}^2 + \omega_m^2] + p_c^2) / \Lambda_{\text{QCD}}^2 \right]} \\ \times \ln \frac{(|\mathbf{p}| - |\mathbf{k}|)^2 + (\omega_n - \omega_m)^2}{(|\mathbf{p}| + |\mathbf{k}|)^2 + (\omega_n - \omega_m)^2} \quad (\text{A1})$$

$$E_2(|\mathbf{p}|, \omega_n; |\mathbf{k}|, \omega_m) = -\frac{8}{27\pi} \cdot \frac{1}{\ln \left[(\max[\mathbf{p}^2 + \omega_n^2, \mathbf{k}^2 + \omega_m^2] + p_c^2) / \Lambda_{\text{QCD}}^2 \right]} \\ \times \left\{ 2 + \frac{\mathbf{p}^2 + \mathbf{k}^2 + 3(\omega_n - \omega_m)^2}{4|\mathbf{p}||\mathbf{k}|} \cdot \ln \frac{(|\mathbf{p}| - |\mathbf{k}|)^2 + (\omega_n - \omega_m)^2}{(|\mathbf{p}| + |\mathbf{k}|)^2 + (\omega_n - \omega_m)^2} \right. \\ \left. + \frac{(\mathbf{p}^2 - \mathbf{k}^2 + (\omega_n - \omega_m)^2)(-\mathbf{p}^2 + \mathbf{k}^2 + (\omega_n - \omega_m)^2)}{4|\mathbf{p}||\mathbf{k}|} \right. \\ \left. \times \left(\frac{1}{(|\mathbf{p}| - |\mathbf{k}|)^2 + (\omega_n - \omega_m)^2} - \frac{1}{(|\mathbf{p}| + |\mathbf{k}|)^2 + (\omega_n - \omega_m)^2} \right) \right\} \quad (\text{A2})$$

$$E_3(|\mathbf{p}|, \omega_n; |\mathbf{k}|, \omega_m) = -\frac{4(\omega_n - \omega_m)}{27\pi|\mathbf{p}||\mathbf{k}|} \cdot \frac{1}{\ln \left[(\max[\mathbf{p}^2 + \omega_n^2, \mathbf{k}^2 + \omega_m^2] + p_c^2) / \Lambda_{\text{QCD}}^2 \right]} \\ \times \left\{ \ln \frac{(|\mathbf{p}| - |\mathbf{k}|)^2 + (\omega_n - \omega_m)^2}{(|\mathbf{p}| + |\mathbf{k}|)^2 + (\omega_n - \omega_m)^2} + (-\mathbf{p}^2 + \mathbf{k}^2 + (\omega_n - \omega_m)^2) \right. \\ \left. \times \left(\frac{1}{(|\mathbf{p}| - |\mathbf{k}|)^2 + (\omega_n - \omega_m)^2} - \frac{1}{(|\mathbf{p}| + |\mathbf{k}|)^2 + (\omega_n - \omega_m)^2} \right) \right\} \quad (\text{A3})$$

$$E_4(|\mathbf{p}|, \omega_n; |\mathbf{k}|, \omega_m) = \frac{4(\omega_n - \omega_m)}{27\pi|\mathbf{p}||\mathbf{k}|} \cdot \frac{1}{\ln \left[(\max[\mathbf{p}^2 + \omega_n^2, \mathbf{k}^2 + \omega_m^2] + p_c^2) / \Lambda_{\text{QCD}}^2 \right]} \\ \times \left\{ \ln \frac{(|\mathbf{p}| - |\mathbf{k}|)^2 + (\omega_n - \omega_m)^2}{(|\mathbf{p}| + |\mathbf{k}|)^2 + (\omega_n - \omega_m)^2} + (\mathbf{p}^2 - \mathbf{k}^2 + (\omega_n - \omega_m)^2) \right. \\ \left. \times \left(\frac{1}{(|\mathbf{p}| - |\mathbf{k}|)^2 + (\omega_n - \omega_m)^2} - \frac{1}{(|\mathbf{p}| + |\mathbf{k}|)^2 + (\omega_n - \omega_m)^2} \right) \right\} \quad (\text{A4})$$

$$E_5(|\mathbf{p}|, \omega_n; |\mathbf{k}|, \omega_m) = \frac{4}{27\pi|\mathbf{p}||\mathbf{k}|} \cdot \frac{1}{\ln \left[(\max[\mathbf{p}^2 + \omega_n^2, \mathbf{k}^2 + \omega_m^2] + p_c^2) / \Lambda_{\text{QCD}}^2 \right]} \\ \times \left\{ -\ln \frac{(|\mathbf{p}| - |\mathbf{k}|)^2 + (\omega_n - \omega_m)^2}{(|\mathbf{p}| + |\mathbf{k}|)^2 + (\omega_n - \omega_m)^2} + 2(\omega_n - \omega_m)^2 \right. \\ \left. \times \left(\frac{1}{(|\mathbf{p}| - |\mathbf{k}|)^2 + (\omega_n - \omega_m)^2} - \frac{1}{(|\mathbf{p}| + |\mathbf{k}|)^2 + (\omega_n - \omega_m)^2} \right) \right\} \quad (\text{A5})$$

- [1] See, for example, H. Satz, Nucl. Phys. **A 681**, 3 (2001); Nucl. Phys. **A 661**, 104 (1999).
- [2] K. Rajagopal, and F. Wilczek, “ The condensed matter physics of QCD ”, hep-ph/0011333.
- [3] K. Rajagopal, in “ *Quark-Gluon Plasma 2* ”, 484-554 (World Scientific, 1995).
- [4] S. Ejiri, Nucl. Phys. Proc. Suppl. **94**, 19 (2001). F. Karsch, Nucl. Phys. Proc. Suppl. **83**, 14 (2000).
- [5] C. D. Roberts, and S. M. Schmidt, Prog. Part. Nucl. Phys. **45S1**, 1 (2000); C. D. Roberts, and A. G. Williams, Prog. Part. Nucl. Phys. **33**, 477 (1994).
- [6] A. Barducci, R. Casalbuoni, S. De Curtis, R. Gatto, and G. Pettini Phys. Rev. **D 41**, 1610 (1990); Phys. Lett. **B 231**, 463 (1989); A. Barducci, R. Casalbuoni, G. Pettini, and R. Gatto, Phys. Rev. **D 49**, 426 (1994).
- [7] M. Harada, and A. Sibata, Phys. Rev. **D 59**, 014010 (1998); D. Blaschke, C. D. Roberts, and S. Schmidt, Phys. Lett. **B 425**, 232 (1998); A. Bender, G. I. Poulis, C. D. Roberts, S. Schmidt, and A. W. Tomas, Phys. Lett. **B 431**, 263 (1998); P. Maris, C. D. Roberts, and S. Schmidt, Phys. Rev. **C 57**, R2821 (1998); K. Fukazawa, T. Inagaki, S. Mukaigawa, and T. Muta, Prog. Theor. Phys. **105**, 979 (2001).
- [8] C. J. Burden, C. D. Roberts, and A. G. Williams, Phys. Lett. **B 285**, 347 (1992); J. I. Skallerud, and A. G. Williams Phys. Rev. **D 63**, 054508 (2001); Nucl. Phys. Proc. Suppl. **83**, 209 (2000).
- [9] P. Jain, and H. J. Munczek, Phys. Rev. **D 44**, 1873 (1991).
- [10] H. Pagels, and S. Stokar, Phys. Rev. **D 20**, 2947 (1979).
- [11] J. M. Cornwall, R. Jackiw, and E. Tomboulis, Phys. Rev. **D 10**, 2428 (1974).
- [12] O. Kiriyama, M. Maruyama, and F. Takagi, hep-ph/0101110; Phys. Rev. **D 62**, 105008 (2000); Phys. Rev. **D 58**, 116001 (1998).
- [13] See, for example, M. Le Bellac, “ *Thermal Field Theory* ” (Cambridge University Press, Cambridge, England, 1996).
- [14] A.G. Williams, G. Krein, and C. D. Roberts, Annals Phys. **210**, 464(1991); P. Jain, and H. Munczek, Phys. Rev. **D 48**, 5403 (1993); Phys. Rev. **D 46**, 438 (1992).
- [15] K. Higashijima, Phys. Rev. **D 29**, 1228 (1984); Prog. Theor. Phys. Suppl. **104**, 1 (1991).
- [16] K. Higashijima, Phys. Lett. **B 124**, 257 (1983); P. Castorina, and S-Y. Pi, Phys. Rev. **D 31**, 411 (1985).
- [17] V. A. Miransky, Sov. J. Nucl. Phys. **38**, 280 (1983).
- [18] P. Maris, and C. D. Roberts, Phys. Rev. **C 56**, 3369 (1997).
- [19] M. R. Frank, and C. D. Roberts, Phys. Rev. **C 53**, 390 (1996).
- [20] A. Höll, P. Maris, and C. D. Roberts, Phys. Rev. **C 59**, 1751 (1999).
- [21] T. Suzuki, Prog. Theor. Phys. **80**, 929 (1989); **81**, 752 (1989); S. Maedan, and T. Suzuki, Theor. Phys. **81**, 229 (1989).
- [22] S. Sasaki, H. Suganuma, and H. Toki, Phys. Lett. **B 387**, 145 (1996); Nucl. Phys. **B 435**, 443 (1995).
- [23] M. Stephanov, K. Rajagopal and E. Shuryak, Phys. Rev. Lett. **81**, 4816 (1998).

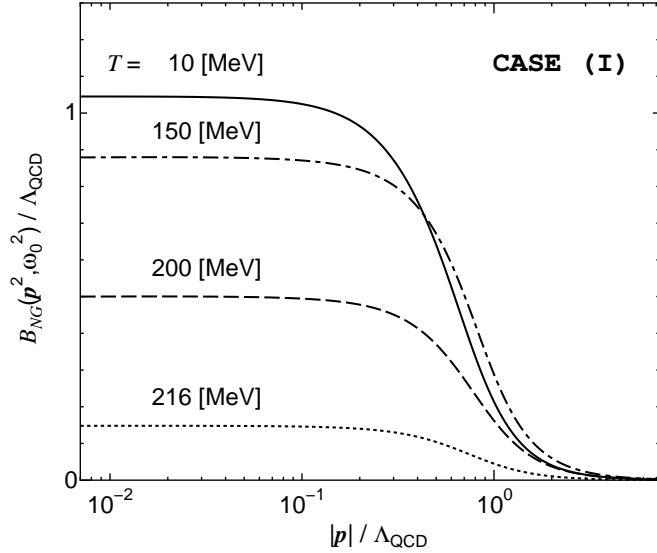


FIG. 1. The momentum dependence of the quark mass-function $B_{NG}(p^2, \omega_0^2)$ in the case (I) at $T = 10, 150, 200$ and 216 MeV with the lowest Matsubara-frequency $\omega_0 = \pi T$.

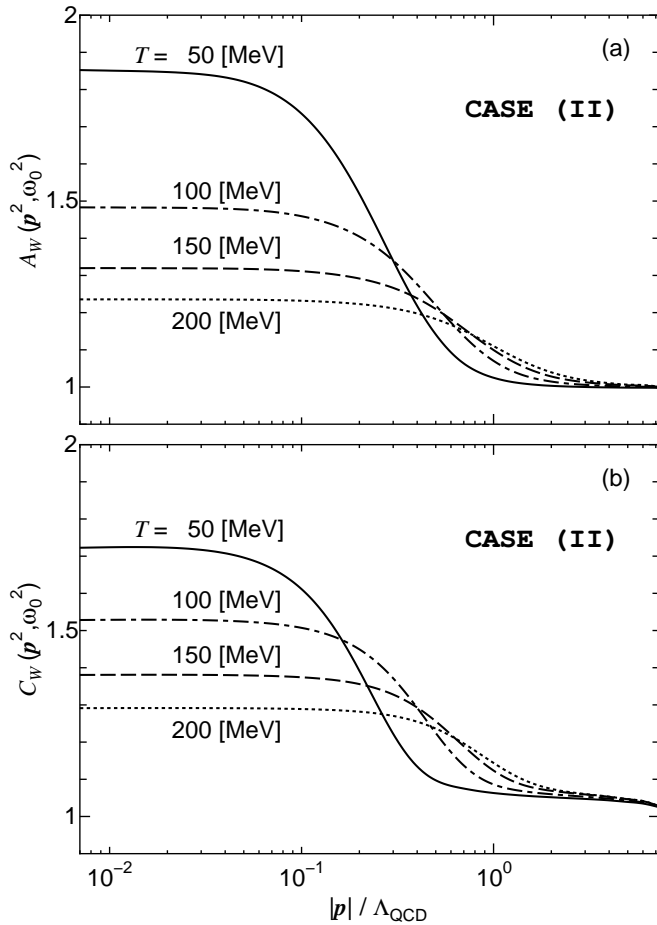


FIG. 2. The momentum dependence of the functions $A_W(p^2, \omega_0^2)$;(a) and $C_W(p^2, \omega_0^2)$;(b) in the case (II) at $T = 50, 100, 150$ and 200 MeV with the lowest Matsubara-frequency $\omega_0 = \pi T$.

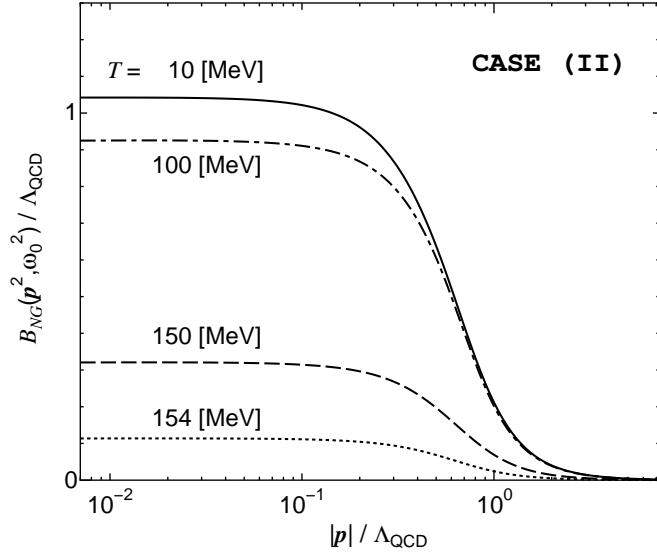


FIG. 3. The momentum dependence of the quark mass-function $B_{NG}(p^2, \omega_0^2)$ in the case (II) at $T = 10, 100, 150$ and 154 MeV with the lowest Matsubara-frequency $\omega_0 = \pi T$.

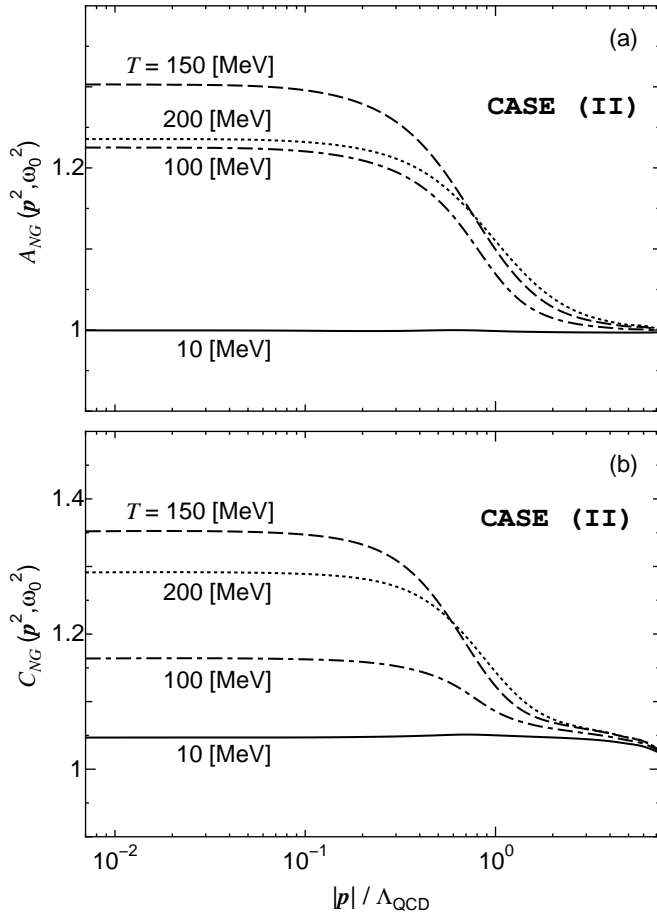


FIG. 4. The momentum dependence of the functions $A_{NG}(p^2, \omega_0^2)$;(a) and $C_{NG}(p^2, \omega_0^2)$;(b) in the case (II) at $T = 10, 100, 150$ and 200 MeV with the lowest Matsubara-frequency $\omega_0 = \pi T$.

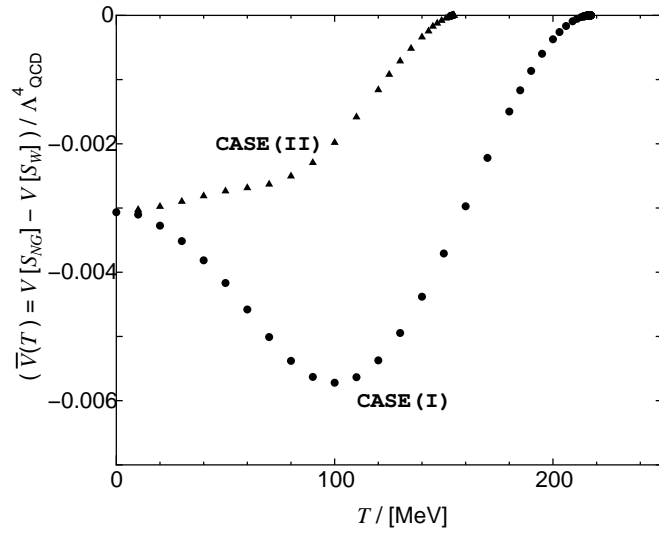


FIG. 5. The temperature dependence of the difference of the effective potential between the NG solution and the Wigner solution. Filled circles show $\bar{V}_{(I)}(T)$ and filled triangles $\bar{V}_{(II)}(T)$.

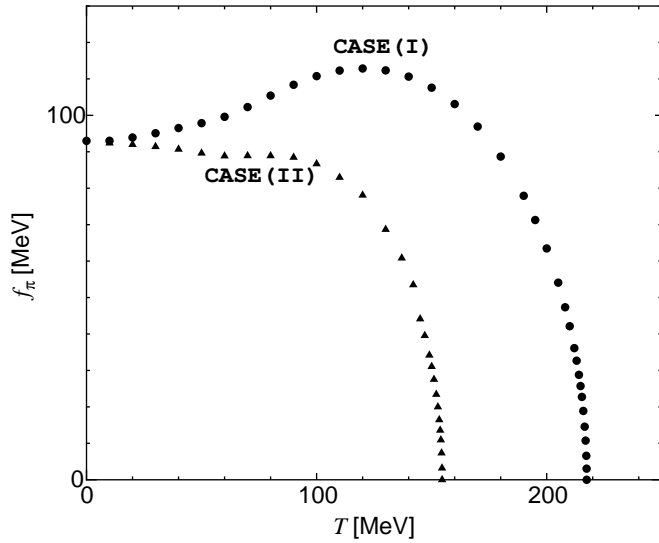


FIG. 6. The temperature dependence of the pion decay constant f_π for the NG solutions in the case (I);(filled circles) and (II);(filled triangles).

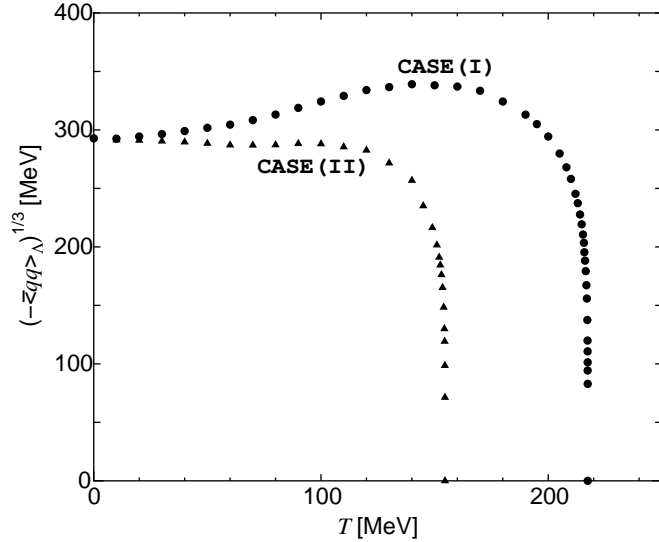


FIG. 7. The temperature dependence of the chiral condensate for the NG solutions in the case (I);(filled circles) and (II);(filled triangles).

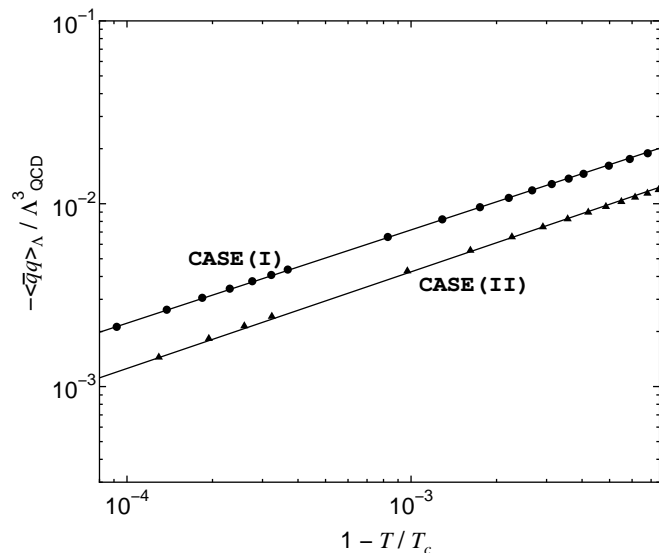


FIG. 8. The temperature dependence of the chiral condensate near the critical temperature T_c for the NG solutions in the case (I);(filled circles) and (II);(filled triangles). $T_c = 217$ MeV in (I) and $T_c = 155$ MeV in (II).